

Apoptosis time window induced by cold atmospheric plasma: comparison with ionizing radiation

Gordana Joksić^{1,*}, Ana Valenta Šobot¹,
Jelena Filipović Tričković¹, Dejan Maletić²,
Nevena Puač², Gordana Malović²,
Zoran Lj. Petrović² and Saša Lazović²

¹Department of Physical Chemistry,
Vinca Institute of Nuclear Sciences, University of Belgrade,
Mike Petrovica Alasa 12-14, 11001 Belgrade, Serbia

²Institute of Physics, University of Belgrade, Pregrevica 118,
11080 Belgrade, Serbia

In this study we evaluate apoptosis time window of primary fibroblasts treated with cold atmospheric plasma (CAP), power range 0.4–1.4 W, for 30 sec, using γ -H2AX phosphorylation assay and flow cytometry. In contrast to irradiation where maximum of γ -H2AX foci appeared 30 min after irradiation and apoptosis 24 h later irrespective of radiation dose, treatment with CAP (power of 0.4 and 0.6) induces maximum of γ -H2AX foci 2 h after treatment. Apoptosis occurred in a power-dependent manner, with time shift of 2–3 h. Besides power-dependent time shift in apoptosis induction, apoptosis time window is the same and lasts for 2 h.

Keywords: Apoptosis, cold atmospheric plasma, ionizing radiation, primary human fibroblasts, repair kinetics.

DOUBLE strand breaks (DSBs) represent the most significant damage of the DNA. In complex reactions between stressor, cellular DNA and repair processes, DNA lesion may be repaired back to the original state, or mis-repaired making chromosomal aberrations or inducing the frame of chromatin structure to activate other cell functions beyond canonical DNA damage response.

Phosphorylated histone H2AX (namely γ -H2AX) represents the first signal molecule in the pathway that activates DSBs repair¹. The role of γ -H2AX foci is to amplify DSB signalling to facilitate cell-cycle arrest at distinct points of the cycle, consecutively enabling sufficient time for repair, namely to prevent entry of damaged cells into mitosis². During the arrest, cells either activate a cascade of proteins needed to complete repair or commit suicide by apoptosis. Phosphorylation of histone H2AX takes place in both processes^{3,4}, representing a universal cellular response to DSBs. Although a body of evidence shows that DSBs could occur after exposure to different exogenous agents, it has also been reported that their molecular structure could be very complex and is strongly relates to their origin, suggesting that their repair

and final fate of cell survival could be strictly related to their complexity^{5,6}.

Cold atmospheric plasma (CAP) produces different kinds of reactive oxygen and nitrogen species (hydroxyl radical (\cdot OH), hydrogen peroxide (H_2O_2), ozone (O_3), atomic oxygen (O), superoxide anion (O_2^-), nitric oxide (NO) and peroxyxynitrite (ONOO^-)), consequently triggering various signalling pathways, including DNA repair, cell cycle control, apoptosis and other types of cell death^{7,8}. In the present study, CAP was generated in a mixture of helium and surrounding air in order to produce reactive oxygen and nitrogen species that play an important role in the plasma–cell interactions. The NO species are generated in the gas phase through several different reaction pathways, including direct reactions involving atomic oxygen and nitrogen atoms, or nitrogen molecule and oxygen atoms. The formation of peroxyxynitrite is possible through several reaction pathways depending on the experimental conditions. It can be formed through reaction of nitrates with hydrogen peroxide or in the reactions with O_2^- and $\text{OH}^{\cdot-}$ (refs 9–11).

Our previous work has shown that the effects of plasma doses can be tuned to match the typical therapeutic doses of ionizing radiation, inducing mainly apoptosis of human primary cells¹². In this study, we have used previously established experimental conditions to further examine the repair kinetics of plasma-induced DSBs as well as to get an approximate estimate of the time window when apoptotic outcome of the cells occurs. Repair kinetics was assessed using γ -H2AX phosphorylation assay and, in parallel, apoptosis was assessed by flow cytometry. The level of lipid peroxidation was also monitored.

Primary fibroblasts were obtained from skin biopsies of three healthy volunteers undergoing plastic surgery. All subjects signed informed consents regarding this study, which conformed to the Declaration of Helsinki and was approved by the Ethical Committee of the Vinca Institute of Nuclear Sciences, Belgrade, Serbia. A total of three primary fibroblast cell lines were established. Cells were grown in Chang Amnio medium (Irvine Scientific, USA) at 37°C in a humid atmosphere and 10% of CO_2 . Each sample was set up in duplicate: one set was used for γ -irradiation while the other set was used for plasma treatment.

As shown in Figure 1, the plasma needle was placed above the samples and powered at 13.56 MHz. Helium flow rate of 1 SLM (standard litre per minute) was used for all treatments. Derivative probes were used to measure the power delivered to the plasma. Grounded electrode made of copper foil was placed beneath the sample-containing vessel. The distance between the needle tip and the samples was 5 mm. Plasma power of 0.4, 0.6 and 1.4 W was used in the experiment. Treatment duration was 30 sec for all three applied powers under standard laboratory conditions, i.e. relative humidity of 50% and

*For correspondence. (e-mail: gjoksic@vin.bg.ac.rs)

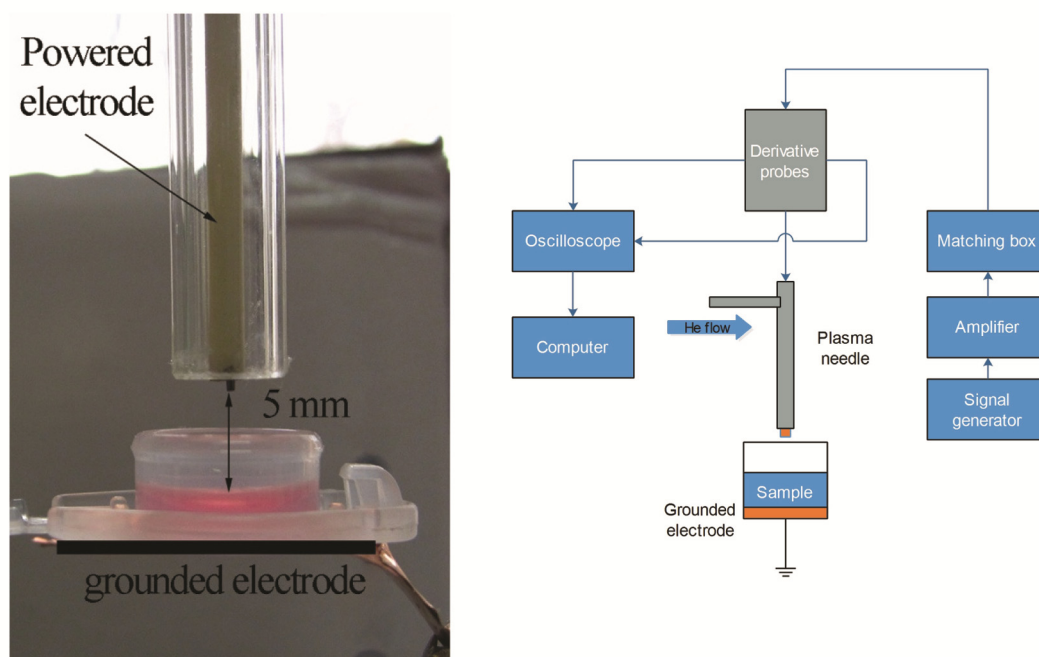


Figure 1. Plasma treatment experimental set-up: photograph and schematic diagram.

temperature of 23°C. The monolayer of cells was covered with 5 μ l of Chang medium; then the cells were placed in an incubator for recovery. To assess the repair kinetics of induced damage slides were processed on different incubation times employing the γ -H2AX phosphorylation assays.

Samples were irradiated using ^{60}Co γ -ray source (the most explored therapeutic dose of 2 Gy at a dose rate 0.45 Gy/min). The dimensions of the radiation field were 20 \times 20 cm and distance from the source was 74 cm. After irradiation, cells were returned to the tissue culture incubator, and processed according to the method of Rogakou *et al.*¹³. Thereafter, the cells were placed in an incubator for recovery. Slides were processed on different incubation times after the treatment (30 min, 2 h, 5 h and 24 h) employing γ -H2AX phosphorylation assay. Parallel samples were used for flow cytometry and lipid peroxidation analysis.

For immunostaining, exponentially growing cells were seeded on polylysine glass slides (Sigma-Aldrich, USA) and allowed to attach to the slide surface for 24 h before treatment with ionizing radiation or cold plasma. At various time points after the treatment (30 min, 2 h, 5 h and 24 h), the cells were fixed in 4% formaldehyde, permeabilized with 0.2% Triton X-100 and stained with the γ -H2AX primary antibody (Merck Millipore, USA) and a FITC-labelled secondary antibody (Sigma-Aldrich, USA). The slides were mounted with 4',6'-diamidino-2-phenylindole (DAPI)-containing Vectashield solution (Vector Laboratories Ltd, UK), covered with coverslips and sealed. Foci positive for γ -H2AX were counted using an epifluorescent Axiomager A1 microscope (Carl Zeiss,

Germany) and the computer software ISIS (Metasystem, Germany), according to the method of Kinner *et al.*¹⁴.

For apoptosis assay, at each time point after irradiation and plasma treatment, cells were washed with pre-warmed phosphate buffer saline (PBS) at 37°C and fixed in 96% ethanol. Apoptosis was monitored by flow cytometry (Becton Dickinson, Germany). DNA content was assessed by measuring the UV fluorescence of propidium iodide-stained DNA (PI, 10 mg/ml, Sigma-Aldrich, USA). Apoptotic population and cell cycle analysis was performed using CellQuest software (Becton Dickinson, Germany), according to the method of Holmes *et al.*¹⁵.

For lipid peroxidation by measuring thiobarbituric acid reactive substances (TBARS) spectrophotometrically, we followed the method of Janero¹⁶: 0.1 ml of pellet and 0.1 ml of medium of the same culture were used for analysis. Briefly, 0.4 ml of 50 mM Tris-HCl buffer containing 180 mM KCl and 10 mM EDTA was added to 0.1 ml of pellet lysate or defrosted medium, 0.5 ml of 2-thiobarbituric acid (Merck; 1 wt%/vol) in 0.05 M NaOH and 0.5 ml of HCl (25 wt%/vol in water). The mixture was heated in boiling water for 10 min, reaction was stopped by cooling samples on ice, and thereafter the chromogen was extracted in 3 ml of *n*-butanol in the organic phase separated by centrifugation at 5000 rpm for 10 min. The absorbance of the organic phase was measured spectrophotometrically (Tecan Sunrise absorbance microplate reader, Tecan Group Ltd, Switzerland) at 532 nm wavelength. The amount of lipid peroxidation was expressed as nmol of TBARS (malondialdehyde, MDA equivalents)/mg of proteins, using a standard curve of 1,1,3,3-tetramethoxypropane. Proteins were

Table 1. Repair kinetics and apoptosis of human primary fibroblasts exposed to non-thermal plasma and ionizing radiation

Treatment	Analysis	0 min	0.5 h	2 h	5 h	24 h
Ionizing radiation	Number of f/c ^a	0.39	19.79	14.53	5.23	1.12
	% of >60 f/c	0.41	8.89	3.47	1.86	0.16
	% of apoptotic cells	9.1	37.25	33.42	25.16	51.51
	MDA ^b (nmol/mg of proteins)	0.54	0.68	0.55	0.33	0.67
CAP ^c power of 0.4 W	Number of f/c	1.39	16.22	39.85	21.8	0.16
	% of >60 f/c	0	1.72	3.9	2.85	0.59
	% of apoptotic cells	8.22	14.43	41.8	31.4	5.82
	MDA (nmol/mg of proteins)	0.54	0.68	0.69	0.8	0.67
CAP power of 0.6 W	Number of f/c	0.4	46.59	47.59	29.27	7.35
	% of >60 f/c	0	42.65	84.9	11.45	0
	% of apoptotic cells	9.14	58.5	68.14	27	0
	MDA (nmol/mg of proteins)	0.59	0.81	0.88	0.74	0.92
CAP power of 1.4 W	Number of f/c	4	13.55	7.88	0	0
	% of >60 f/c	0	36.15	76.08	0	0
	% of apoptotic cells	9.4	36.1	68	0	0
	MDA (nmol/mg of proteins)	0.79	1.47	1.45	1.23	1.3

^af/c, γ -H2AX focus per cell. ^bMDA, Malondialdehyde. ^cCAP, Cold atmospheric plasma.

determined according to Lowry *et al.*¹⁷ using bovine serum albumin as standard.

Statistical analysis was performed using SPSS 10 for Windows. Differences between the groups were assessed using nonparametric Mann Whitney *U* test, while correlation between different parameters was assessed by Pearson correlation. Differences at $P < 0.05$ were accepted as the level of significance.

Table 1 and Figure 2 present results obtained in the experiment where cells were directly exposed to non-thermal plasma.

Previously established experimental parameters such as power delivered to plasma of 0.4, 0.6 and 1.4 W and exposure time of 30 sec, were used to study repair kinetics of DSBs (visualized by γ -H2AX histone), apoptosis and lipid peroxidation biomarker – MDA at different recovery periods after treatment. Results were compared with the effects of γ -rays (⁶⁰Co) – acute irradiation. The power of 0.4, 0.6 and 1.4 W corresponds to voltage 337, 357 and 393 V respectively. At exposure time of 30 sec calculated corresponding equivalent radiation dose ranged from 0.96 (0.4 W and 30 sec) to 2.2 Gy (ref. 12).

The baseline level of γ -H2AX in unexposed control cells was 3.9 per cell, whereas 30 min after plasma treatment (power of 0.4 W), the yield of γ -H2AX reached 16.2 foci per cell. Further increase in power (0.6 W) induced 46.6 foci per cell, whereas power of 1.4 W momentarily induced cell death seen as misshapen nuclei (Figure 2a and b) or as a ‘track’ (Figure 2a) where all the cells closest to the powered electrode were detached from the polylysine surface.

A maximum of foci induction after non-thermal plasma treatment with power of 0.4 and 0.6 W occurred 2 h after treatment (1.5 h later when compared with ionizing radiation), indicating that most of the treated cells will die

via apoptosis (Table 1). Initial DNA damages are non-reparable and determine early apoptosis. This observation was confirmed by flow cytometry data, which showed that apoptosis occurred in a dose (power)-dependent manner, i.e. the highest power induced necrosis, power of 0.6 W induced apoptosis with maximum between 30 min and 2 h after treatment; whereas 0.4 W induced apoptosis 2 h after exposure and last continuously for up to 5 h (Table 1). Interestingly, besides power-dependent time shift in apoptosis induction, apoptosis time window was the same and lasted for 2 h.

A positive correlation between the number of cells carrying 60 signals per cell and percentage of cells displaying apoptotic granulation was found for cold plasma treatments with power of 0.4 and 0.6 W (Pearson correlation, $P < 0.01$, $r = 0.967$ and $P < 0.05$, $r = 0.934$ respectively). In samples treated with power of 1.4 W, high number of misshapen nuclei was observed, as well as elevated concentration of MDA. Bulky phosphorylation of γ -H2AX seen as more than 60 signals per nuclei, correlates with apoptotic fragmentation. It has been previously reported that H2AX phosphorylation that leads to apoptosis mainly occurred by DNA-PKcs⁴, although phosphorylation of H2AX via c-Jun N terminal kinases (JNK) cannot be neglected due to UV irradiation in plasma source. However, DNA-PKcs are predominant kinases that phosphorylate H2AX when irreparable lesions are induced, activating apoptosis, as revealed by the normal fibroblast cell lines that we used in the experiment. In cells irradiated with ionizing radiation, phosphorylation of H2AX occurs via ATM kinase that leads to activation of cascade molecules involved in DSBs repair. H2AX is the most important molecule in a switch between apoptosis versus repair response following DNA damage^{18,19}. According to the results obtained in this

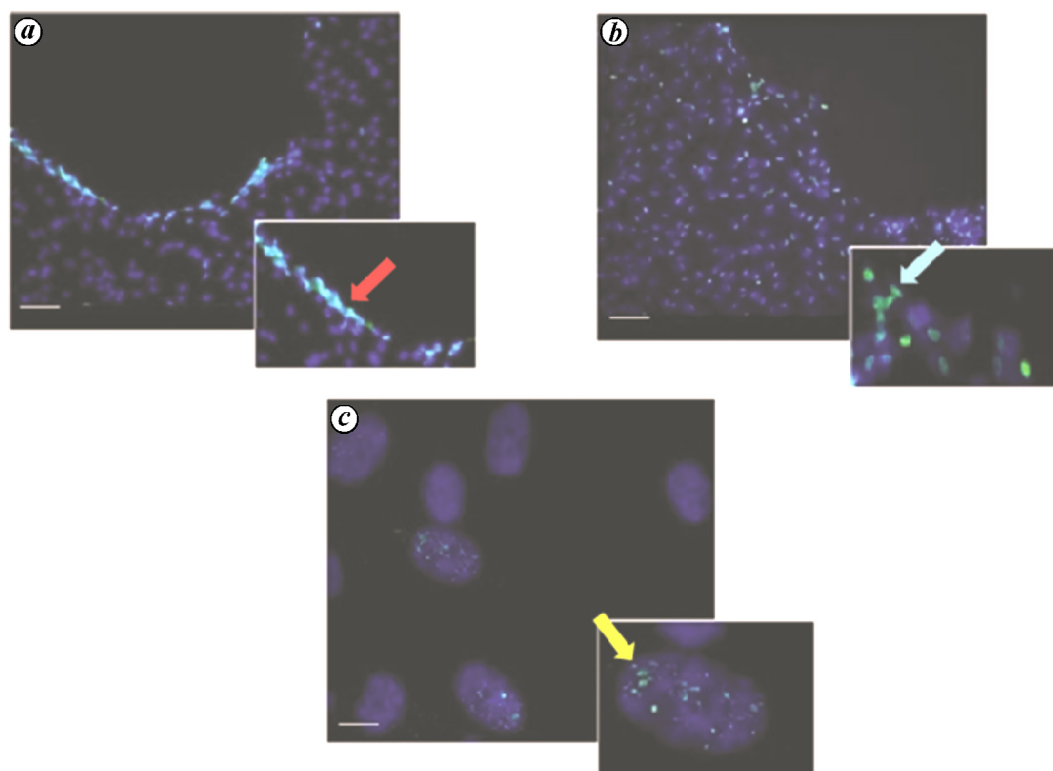


Figure 2. Photomicrographs of plasma and ionizing radiation-treated cells visualized by immunostaining. *a, b*, Cold plasma-treated samples, power 1.4 W. In (*a*), red arrow indicates detached cells seen as a 'track'. In (*b*), blue arrow indicates FITC-labelled necrotic cells; scale bar = 150 μm . *c*, Ionizing radiation-treated cells. Yellow arrow indicates $\gamma\text{-H2AX}$ foci in FITC-labelled cells; scale bar = 30 μm .

study, we can conclude that non-thermal atmospheric plasma power (0.4–0.6 W) predominantly induces apoptosis, whereas power of 1.4 W predominantly induces necrosis (Figure 2 *a* and *b*).

Treatment with ionizing radiation (^{60}Co γ -rays) induces maximum $\gamma\text{-H2AX}$ foci formation 30 min after irradiation, 19.79 (Table 1, Figure 2 *c*). Induced DSBs are mostly repaired within 24 h. During recovery period, a portion of cells undergoes unsuccessful repair outcome, and is removed from the population via apoptosis. Apoptosis starts 30 min after irradiation (37.25%) and continuously occurs during the next 5 h almost at the same extent, suggesting that all cells that enter the S-phase of the cell cycle with unrepaired DSBs are directed towards apoptosis. The maximum pick of apoptosis takes place 24 h after irradiation (51.51%), restoring $\gamma\text{-H2AX}$ foci mostly to the baseline level. Residual foci, after recovery period of 24 h, are the main side effects after irradiation with ionizing radiation, because unrepaired DSBs can interact with other lesions creating hybrid genes, deletion or duplication that can lead to genomic instability and transformation of cells^{8,20}.

In contrast to ionizing radiation, treatment with cold plasma power of 0.4 and 0.6 W induces maximum formation of $\gamma\text{-H2AX}$ foci 2 h after treatment, accompanied by massive apoptosis of treated cells (Table 1). The highest

power (1.4 W) induces necrosis of cells, characterized with misshapen, sparkling, partly detached nuclei, as seen microscopically. MDA levels were also elevated in these cells; they were statistically significant compared with other treatments ($P < 0.05$), indicating increased lipid peroxidation (Table 1). Lipid peroxidation, depending on its extent, may endorse cellular survival or lead to cell death. High peroxidation rates that overcome repair capacities result in cell death^{21,22}, which, accompanied with exhausted energetic capacities, directs cells to necrosis²³. After recovery period of 24 h, the number of cells surviving after treatment with non-thermal plasma power of 1.4 W is low, suggesting that initially induced bulky lesions determine lethal fate of treated cells.

Non-thermal plasma is a promising method to be used for treatment of small tissue areas. The results of this study strongly indicate that non-thermal plasma treatment in the power range 0.4–0.6 W induces apoptosis, whereas further increase in power induces massive irreparable lesions which lead to necrosis. Power-dependent time shift in apoptosis is observed, while apoptosis time window remains the same and lasts for 2 h. Further studies on non-thermal plasma should be directed towards examining the possible bystander effects on the surroundings of target tissues, since extracellular liquid of treated tissues carries newly produced chemical compounds that

can be stable for certain periods of time and induce adverse effects to the surrounding tissues acting as chemical messengers.

Conflict of interest: The authors declare no conflicts of interest.

1. Downs, J. A., Lowndes, N. F. and Jackson, S. P., A role for *Saccharomyces cerevisiae* histone H2A in DNA repair. *Nature*, 2000, **408**, 1001–1004.
2. Downs, J. A. *et al.*, Binding of chromatin-modifying activities to phosphorylated histone H2A at DNA damage sites. *Mol. Cell*, 2004, **16**, 979–990.
3. Rogakou, E. P., Nieves-Neira, W., Boon, C., Pommier, Y. and Bonner, W. M., Initiation of DNA fragmentation during apoptosis induces phosphorylation of H2AX histone at serine 139. *J. Biol. Chem.*, 2000, **275**, 9390–9395.
4. Yuan, J., Adamski, R. and Chen, J., Focus on histone variant H2AX: to be or not to be. *FEBS Lett.*, 2010, **584**, 3717–3724.
5. Schipler, A. and Iliakis, G., DNA double-strand break complexity levels and their possible contributions to the probability for error-prone processing and repair pathway choice. *Nucleic Acids Res.*, 2013, **41**, 7589–7605.
6. Shibata, A. *et al.*, Factors determining DNA double-strand break repair pathway choice in G2 phase. *EMBO J.*, 2011, **30**, 1079–1092.
7. Dezest, M. *et al.*, Mechanistic insights into the impact of cold atmospheric pressure plasma on human epithelial cell lines. *Sci. Rep.*, 2017, **7**, 41163.
8. Noda, A., Radiation-induced unreparable DSBs: their role in the late effects of radiation and possible applications to biodosimetry. *J. Radiat. Res.*, 2018, **59**, ii114–ii120.
9. Bruggeman, P. J. *et al.*, Plasma–liquid interactions: a review and roadmap. *Plasma Sources Sci. Technol.*, 2016, **25**, 053002.
10. Lukes, P., Dolezalova, E., Sisrova, I. and Clupek, M., Aqueous-phase chemistry and bactericidal effects from an air discharge plasma in contact with water: evidence for the formation of peroxynitrite through a pseudo-second-order post-discharge reaction of H₂O₂ and HNO₂. *Plasma Sources Sci. Technol.*, 2014, **23**, 015019.
11. Seth, A. N., Wei, T., Eric, J. and Mark, J. K., Atmospheric pressure plasma jets interacting with liquid covered tissue: touching and not-touching the liquid. *J. Phys. D.*, 2014, **47**, 475203.
12. Lazović, S. *et al.*, Plasma induced DNA damage: comparison with the effects of ionizing radiation. *Appl. Phys. Lett.*, 2014, **105**, 124101.
13. Rogakou, E. P., Pilch, D. R., Orr, A. H., Ivanova, V. S. and Bonner, W. M., DNA double-stranded breaks induce histone H2AX phosphorylation on serine 139. *J. Biol. Chem.*, 1998, **273**, 5858–5868.
14. Kinner, A., Wu, W., Staudt, C. and Iliakis, G., Gamma-H2AX in recognition and signaling of DNA double-strand breaks in the context of chromatin. *Nucleic Acids Res.*, 2008, **36**, 5678–5694.
15. Holmes, K. L., Otten, G. and Yokoyama, W. M., Flow cytometry analysis using the Becton Dickinson FACS Calibur. In *Current Protocols in Immunology* (eds Coligan, J. E. *et al.*), John Wiley, USA, 2002, vol. 49, pp. 5.4.1–5.4.22.
16. Janero, D. R., Malondialdehyde and thiobarbituric acid-reactivity as diagnostic indices of lipid peroxidation and peroxidative tissue injury. *Free Radic. Biol. Med.*, 1990, **9**, 515–540.
17. Lowry, O. H., Rosebrough, N. J., Farr, A. L. and Randall, R. J., Protein measurement with the Folin phenol reagent. *J. Biol. Chem.*, 1951, **193**, 265–275.
18. Cook, P. J., Ju, B. G., Telese, F., Wang, X., Glass, C. K. and Rosenfeld, M. G., Tyrosine dephosphorylation of H2AX modulates apoptosis and survival decisions. *Nature*, 2009, **458**, 591.
19. Xiao, A. *et al.*, WSTF regulates the H2AX DNA damage response via a novel tyrosine kinase activity. *Nature*, 2009, **457**, 57–62.
20. Fenech, M., The cytokinesis-block micronucleus technique: a detailed description of the method and its application to genotoxicity studies in human populations. *Mutat. Res.*, 1993, **285**, 35–44.
21. Ayala, A., Munoz, M. F. and Arguelles, S., Lipid peroxidation: production, metabolism, and signaling mechanisms of malondialdehyde and 4-hydroxy-2-nonenal. *Oxid. Med. Cell. Longev.*, 2014, **2014**, 360438.
22. Haghdoost, S., Sjolander, L., Czene, S. and Harms-Ringdahl, M., The nucleotide pool is a significant target for oxidative stress. *Free Radic. Biol. Med.*, 2006, **41**, 620–626.
23. Vairetti, M., Ferrigno, A., Bertone, R., Richelmi, P., Berte, F. and Freitas, L., Apoptosis vs necrosis: glutathione-mediated cell death during rewarming of rat hepatocytes. *Biochim. Biophys. Acta*, 2005, **1740**, 367–374.

ACKNOWLEDGEMENTS. We thank Dr Miroslav Demajo, Vinca Institute of Nuclear Science University of Belgrade for critically reading the manuscript. This work is financially supported by the Ministry of Education, Science and Technological Development of the Republic of Serbia, Grant No. 173046.

Received 5 October 2018; revised accepted 27 December 2018

doi: 10.18520/cs/v116/i7/1229-1233

Indole-3-acetic acid production by the cyanobacterium *Fisherella muscicola* NDUPC001

S. K. Mishra, Jyoti Singh, Astha Raj Pandey and N. Dwivedi*

Department of Botany, U.P. College (Autonomous), Varanasi 221 002, India

Fisherella muscicola* NDUPC001 was isolated from agricultural fields of Varanasi, India. The cyanobacterial strain was characterized by morphological as well as molecular methods (16S rRNA gene with accession no. JX876898.2) and was deposited at NAIMCC (NBAIM), Mau, Uttar Pradesh, India (accession no. NAIMCC-C-000121). The cyanobacterial strain produced tryptophan-dependent indole-3-acetic acid (IAA), which was identified by thin-layer chromatography and quantitative determination was done by Salkowski's colorimetric method. The maximum amount of IAA production was 286.82 µg/ml on the 19th day in culture medium supplemented with 5 mg/ml of L-tryptophan. The cyanobacterial extract increased the length of radicle, plumule and number of adventitious roots of rice several times in comparison to control to state the IAA production by *Fisherella

*For correspondence. (e-mail: drnagendra.dwivedi@gmail.com)